JOURNAL OF BACTERIOLOGY, Nov. 1989, p. 5803–5811
0021-9193/89/115803-09$02.00/0

Vol. 171, No. 11

Mechanism of Erythromycin-Induced *ermC* mRNA Stability in *Bacillus subtilis*

DAVID H. BECHHOFER* AND KEVIN H. ZEN

Department of Biochemistry, Mount Sinai School of Medicine, New York, New York 10029

Received 31 May 1989/Accepted 10 August 1989

In *Bacillus subtilis*, the *ermC* gene encodes an mRNA that is unusually stable (40-min half-life) in the presence of erythromycin, an inducer of *ermC* gene expression. A requirement for this induced mRNA stability is a ribosome stalled in the *ermC* leader region. This property of *ermC* mRNA was used to study the decay of mRNA in *B. subtilis*. Using constructs in which the ribosome stall site was internal rather than at the 5′ end of the message, we show that ribosome stalling provides stability to sequences downstream but not upstream of the ribosome stall site. Our results indicate that *ermC* mRNA is degraded by a ribonucleolytic activity that begins at the 5′ end and degrades the message in a 5′-to-3′ direction.

Control of mRNA stability can play a major role in the posttranscriptional regulation of procaryotic gene expression. The expression of several genes in polycistronic transcription units is known to be regulated at the level of differential mRNA stability (2, 4, 37). However, little is known about the mechanism(s) for degrading mRNA.

That 3′-to-5′ exonucleases are involved in mRNA decay is implied by the finding that mRNA sequences at the 3′ end or at intercistronic regions appear to act as barriers to decay (for reviews, see references 8 and 27; see also reference 11). It has been shown that the chemical half-lives of specific mRNAs are increased in *Escherichia coli* strains bearing mutations in two genes that encode 3′-to-5′ exoribonucleases, polynucleotide phosphorylase, and RNase II (1, 14). Others have reported the detection in vivo of decay intermediates with various 5′ ends, suggesting that mRNA is rendered functionally inactive by site-specific endonucleolytic cleavages (9, 33, 38, 46). It has been demonstrated recently that endonucleolytic cleavage by RNase III is the initial step in the decay of the polynucleotide phosphorylase message (39). A 5′-to-3′ exoribonuclease has not been identified in *E. coli* (12).

Despite the presence of many RNases in *E. coli*, mRNAs can nevertheless be stabilized by specific mRNA sequences at the 5′ end (5, 18). These sequences confer *cis*-dominant stability to otherwise unstable mRNA segments, indicating that a limited number of sites determines the instability of a particular mRNA. Although mRNA stability has been attributed to occupancy by ribosomes (9), untranslated regions of mRNA are not necessarily more labile than translated regions (5, 31).

We chose the *ermC* gene, which is carried on plasmid pE194 in *Bacillus subtilis*, as a model to study the factors involved in mRNA stability in this organism. The *ermC* gene encodes an rRNA methyltransferase (methylase) (42) that confers macrolide-lincosamide-streptogramin B resistance on the host by reducing the affinity of ribosomes for these antibiotics (44, 49). Expression of the *ermC* gene product is induced in the presence of subinhibitory concentrations of erythromycin, a macrolide-lincosamide-streptogramin B antibiotic, by a translational attenuation mechanism (15, 48). In the absence of erythromycin, the *ermC* mRNA leader sequence is folded in a stable stem-loop structure such that the ribosome-binding site preceding the methylase-coding sequence (Shine-Dalgarno sequence 2 [SD2]) is unavailable for translation. In the presence of erythromycin, an erythromycin-bound ribosome stalls while translating the 19-amino-acid leader peptide, thereby opening the stem-loop structure to allow ribosome binding at SD2. Induction by erythromycin results in a 20-fold increase in methylase translation. This induction is accompanied by a 15- to 20-fold increase in *ermC* mRNA stability (3, 44). Induced *ermC* mRNA stability is independent of translation of the methylase-coding sequence but requires translation of the leader peptide. Several RNAs that have the 5′ end (360 nucleotides) of *ermC* and diverse 3′ ends are also stabilized in the presence of erythromycin, indicating that the 5′ segment of *ermC* mRNA confers *cis*-dominant stability. Similar results have been reported recently for another erythromycin resistance gene, *ermA* (41).

We have proposed several ways by which a stalled ribosome can stabilize *ermC* mRNA (3). The simplest model is that the ribosome physically protects the mRNA from RNase attack. Decay of *ermC* mRNA could be initiated by endonucleolytic cleavage in the leader peptide sequence where the ribosome stalls. Recent genetic evidence suggests that the stall site is upstream of leader peptide codon 10 (32). Alternatively, the 5′ terminus of the message could be the target for initiation of processive decay in the 5′-to-3′ direction. A stalled ribosome in the leader peptide could cause stalling of another ribosome loading at the ribosome-binding site for the leader peptide (SD1) such that the 5′ end of *ermC* mRNA, which is only 9 nucleotides upstream of SD1, is protected. It has been shown in vitro that erythromycin-induced ribosome stalling in the *ermC* leader peptide results in RNase protection of the 5′ end of the message (36). A different model for the stabilizing effect of a stalled ribosome is that an erythromycin-induced conformational change in the leader region mRNA masks an RNase target site, which is distal to the site of ribosome stalling.

We constructed insertion mutations of the *ermC* leader region that were designed to examine how ribosome stalling affects *ermC* mRNA stability. Our results suggest strongly that *ermC* mRNA is degraded primarily in the 5′-to-3′ direction by a ribonucleolytic activity that starts at the 5′ end, and that a stalled ribosome at the 5′ end protects against this type of decay. These results explain how ribosome

* Corresponding author.

TABLE 1. Bacterial strains and plasmids used in this study

B. subtilis strain or plasmid	Genotype	Source or reference
Strain		
IS75	*hisA1 leu metB5*	I. Smith
BD170	*trpC2 thr-5*	D. Dubnau
CU403	*thyA thyB metB5 divIVBI*	40
Plasmids		
pBD142	Em^r Cm^r	3
pSD100	pBD142 containing a tandem repeat of the 275-base-pair *AluI* fragment of pC194, inserted upstream of SD1	This work
pBD9	pE194-pUB110 composite joined at their *XbaI* sites	23
pBD118	pBD9 with the *ermC* promoter deleted	23
pBD362	pBD118 with the pUB110 replication origin deleted	This work
pBD178	pBD9 with the *ermC* promoter and SD1 deleted	23
pSD132	pSD100 derivative containing two ribosome stall sites	This work

stalling in the *ermC* leader region can provide stability to diverse downstream RNA sequences.

MATERIALS AND METHODS

Bacterial strains. The bacterial strains used in this study are described in Table 1. The host for plasmid pSD100 and its derivatives and for plasmid pBD362 was IS75. BD170 was the host for plasmid pBD178. The *B. subtilis* minicell-producing host was CU403 (40).

Standard procedures. The preparation of *B. subtilis* growth media and competent *B. subtilis* cultures was as described previously (16). Isolation of plasmid DNA and transformation were as described previously (20). Plasmids were introduced into the minicell strain CU403 by transformation. Isolation of minicells, labeling, and sodium dodecyl sulfate-polyacrylamide gel analysis of plasmid-encoded polypeptides were exactly as described previously (43).

Plasmids. Plasmid pSD100 is a derivative of plasmid pBD142. Plasmid pBD142 consists of pE194 *cop-6* (21) plus the chloramphenicol resistance determinant of pC194 on a *ClaI* fragment. A synthetic 30-base-pair fragment, prepared by B. Goldschmidt of the Department of Biochemistry, New York University Medical School (New York, N.Y.), consisted of the following sequence:

```
          <−10>          <PvuII>
5′-CGTGCTATAATTATACTAATCAGCTGAGCT-3′
   TCGAGCACGATATTAATATGATTAGTCGAC
```

This fragment, which has overlapping *SacI* ends, was cloned into the pBD142 *SacI* site, which is located between the *ermC* −10 and −35 promoter sequences. The −10 sequence in the inserted fragment was the proper distance from the upstream −35 sequence, and the original *ermC* −10 sequence was still present downstream of the inserted fragment. The pBD142 derivative that contained the inserted 30-base-pair fragment was pSD1. By reverse transcriptase analysis, we found that *ermC* mRNA encoded by pSD1 has two transcriptional start sites 30 nucleotides apart. Apparently, the original *ermC* −10 sequence, although it does not have a proper −35 sequence upstream of it, can promote transcription of *ermC* in this construct. To avoid the problem of two *ermC* RNAs, the original *ermC* −10 sequence was inactivated by using oligonucleotide-directed mutagenesis (29) to change the −10 region sequence (TATAATTATA) to an *Eco*RI site (GAATTC).

The unique *PvuII* site present on the inserted 30-base-pair fragment was used to clone isolated *AluI* fragments of pC194. One clone chosen for further study (plasmid pSD100) contained a tandem insert of a 275-base-pair *AluI* sequence, which consists of nucleotides 2711 to 2437 of the published pC194 sequence (25). Although the published sequence does not have an *AluI* site at nucleotide 2711, restriction endonuclease mapping of pC194 revealed that there was a *PvuII* site (which is also an *AluI* site) at that position. The C-G base pair at position 2711 in the published sequence must therefore be incorrect. The orientation of the inserted *AluI* fragments was determined by the asymmetric *TaqI* site (see Fig. 2). Upon *MboI* digestion of some preparations of pSD100 and pSD132 DNAs, we observed an additional minor band that represented a small deletion of the inserted pC194 DNA. This probably arose because the insert is a tandem repeat. An internal deletion of this sort could explain the intermediate-sized RNAs detected in the blot analyses of pSD100- and pSD132-encoded *ermC* mRNAs.

The *Bal* 31-deleted plasmid used for the experiment for which the results are shown Fig. 3C was made by digesting pSD100 with *PvuII*, treating it briefly with *Bal* 31, and religating. Plasmid molecules that had small deletions were isolated, and one of these, pSD125, was chosen for further study. An *MboI* fragment from pSD125 (*MboI-BclI* in Fig. 2), which contained the upstream sequence of pSD100 (minus a 25-base-pair deletion) and the first 360 nucleotides of *ermC*, was cloned into the *Bam*HI site of M13mp18 for sequencing.

To construct plasmid pSD132 (see Fig. 6), we used plasmid pBD452, which was kindly provided by F. Breidt of the Public Health Research Institute of New York (New York, N.Y.). Plasmid pBD452 is a derivative of pBD142 that has a *SalI* linker inserted 6 nucleotides downstream from the end of the *ermC* leader peptide-coding sequence. A *SalI-HaeIII* digest of pBD452 yielded three fragments, the smallest of which represented the 5′ end of the methylase-coding sequence. The two larger *SalI-HaeIII* fragments of pBD452 were gel purified and ligated with a *SalI-HaeIII* fragment from the replicative form of M13mp18 DNA that contained the pSD125 *MboI* fragment (see above). A plasmid, pSD132, was recovered that had the promoter and 5′ end of *ermC* up to the *SalI* site of pBD452, followed by the upstream sequence of pSD125, followed by the wild-type *ermC* leader region and the methylase-coding sequence. The sequence between the 5′-proximal and the internal ribosome stalling sites in pSD132 was identical to the upstream sequence of pSD100, except for the 25-base-pair deletion present in pSD125.

Construction of plasmids pBD118 (deletion 14) and pBD178 (deletion 83) has been described by Hahn et al. (23). Plasmid pBD118 has a pUB110 (high-copy-number) and a pE194 (low-copy-number) replicon. Plasmid pBD362, the low-copy-number version of pBD118, was constructed by digesting pBD118 at its unique *NcoI* site, which is located in the pUB110 replication region, followed by brief *Bal* 31 digestion and religation. This inactivated the pUB110 replicon, and replication of pBD362 was from the pE194 replicon.

Analysis of RNA. RNA isolation and Northern blot analysis were performed as described previously (3). For RNA gels, the amount of total RNA per lane (approximately 3 μg) varied by less than 20%, as judged by ethidium bromide

staining and visualization of rRNA bands under UV light. In control experiments, our standard concentration of single-stranded probe was in excess of the concentration of *ermC* mRNA, for at least 45 μg of total RNA.

Reverse transcriptase analysis was performed essentially as described by Graves and Rabinowitz (19). The oligonucleotide primer for these experiments was fragment 2 of Narayanan and Dubnau (36). A total of 50 μg of RNA was denatured at 65°C for 10 min in a 14-μl volume containing 50 mM Tris hydrochloride (pH 8.0), 8 mM $MgCl_2$, 30 mM KCl, 1 mM dithiothreitol, 5 ng of end-labeled primer, and 25 U of RNase inhibitor (Boehringer Mannheim Biochemicals, Indianapolis, Ind.). After an additional 4 min at 42°C, deoxynucleoside triphosphates (final concentration, 0.5 mM) and 12 U of avian myeloblastosis virus reverse transcriptase (Life Sciences, Inc., St. Petersburg, Fla.) were added, and incubation was continued at 42°C for 35 min. The reaction was stopped by the addition of EDTA (50 mM) and extracted with an equal volume of phenol-chloroform (1:1). Nucleic acid was precipitated by adding 0.5 volume of ammonium acetate and two volumes of ethanol. The dried pellet was suspended in 4 μl of a DNA sequencing dye mix, heated to 80°C for 2 min, and run on an 8% polyacrylamide–8 M urea sequencing gel. The same primer (unlabeled) was used for dideoxy sequencing of a single-stranded DNA template containing the coding strand.

Quantitation of mRNA half-lives was performed by analyzing autoradiograms of Northern blots on a densitometer (UltroScan XL; LKB Instruments, Inc., Rockville, Md.).

RESULTS

Induced *ermC* mRNA stability is not a result of processing at the 5′ end. Although the size of stable *ermC* mRNA, as detected by Northern blot analysis, appears to be the same as that of unstable *ermC* mRNA (3), we could not exclude the possibility that induced stability of *ermC* mRNA was due to processing at the 5′ end. Krisch and colleagues (6, 34) have shown that stabilization of bacteriophage T4 gene *32* mRNA is a result of processing at the 5′ end that removes 70 nucleotides of the initial transcript. To determine the 5′ end of stable *ermC* mRNA, an oligonucleotide complementary to the *ermC* leader mRNA was annealed and extended by reverse transcriptase (Fig. 1). The results showed identical 5′ ends for uninduced (unstable) and induced (stable) *ermC* mRNA templates. Therefore, induced *ermC* mRNA stability is not a consequence of processing at its 5′ end.

Construction of a mutant in which SD1 is distal from the 5′ end of *ermC* mRNA. As mentioned above, one explanation for the stabilizing effect of a stalled ribosome is protection of the 5′ end of *ermC* mRNA from a processive 5′-to-3′ degradation. We reasoned that if *ermC* mRNA decay from the 5′ end is blocked by the presence of a ribosome stalled at the leader peptide ribosome-binding site (SD1), then the positioning of SD1 far downstream of the 5′ end would allow us to detect the differential stability of RNA sequences upstream and downstream of the ribosome stall site.

To address this point, plasmid pSD100 was constructed (Fig. 2). A synthetic 30-base-pair fragment with *Sac*I ends was inserted into the *Sac*I site, which is located between the −35 and −10 *ermC* promoter sequences. The 30-base-pair insert restored the native *ermC* promoter sequence (see Materials and Methods) and contained a new *Pvu*II site, which was used to clone isolated *Alu*I fragments from plasmid pC194. One clone was selected that contained a tandem insert of a 275-base-pair *Alu*I fragment in the *Pvu*II site, yielding plasmid pSD100. Based on its nucleotide sequence (nucleotides 2711 to 2437 of pC194 [25]), this inserted fragment did not appear to contain any transcriptional or translational signals that could complicate the analysis. SD1 was located 580 nucleotides downstream of the transcriptional start site in pSD100-encoded *ermC* mRNA. Methylase expression from pSD100 was inducible by erythromycin (Fig. 3A); thus, ribosome stalling occurs normally in this construct.

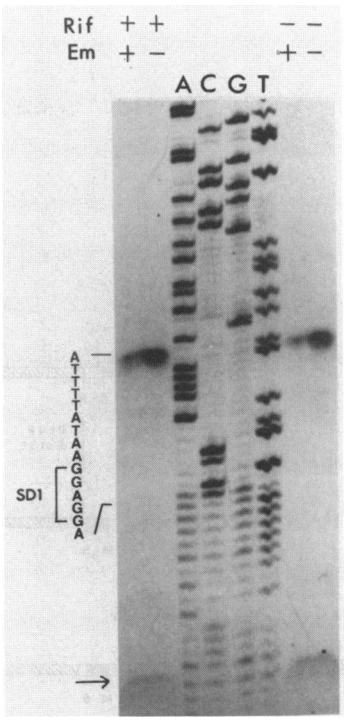

FIG. 1. Mapping the 5′ end of unstable and stable *ermC* mRNAs. Reverse transcriptase was used to extend an oligonucleotide primer annealed to the *ermC* leader peptide sequence. RNA was isolated from a strain containing wild-type *ermC* in the absence of erythromycin (Em) or 15 min after the addition of erythromycin to 0.02 μg/ml. To control for subsequent Northern blot experiments, in which decay of *ermC* mRNA was assayed after the addition of rifampin (Rif), the 5′ end was mapped also in the presence or absence of rifampin. The middle four lanes are a dideoxy sequencing ladder of the *ermC* leader region with the same oligonucleotide primer as was used in the reverse transcriptase reactions. The template for the sequencing reactions was M13 single-stranded DNA containing the coding strand of the *ermC* *Sac*I-*Bcl*I fragment (see Fig. 2). To the left is the sequence of the coding strand, showing that the 5′ end is 9 nucleotides from SD1, as has been determined previously by RNA sequencing (35). The arrow marks the position of the end-labeled primer.

Analysis of pSD100-encoded *ermC* mRNA. RNA was isolated from the pSD100 strain in the presence and absence of erythromycin at various times after rifampin addition (Fig. 3B). The probe, which was complementary to sequences downstream of the *ermC*-proximal *Sac*I site (5′ end probe), detected 1,400-nucleotide (large) and 900-nucleotide (small) RNA fragments at the time of addition of rifampin. Both of these RNAs were unstable in the absence of erythromycin. In the presence of erythromycin, however, the large RNA was unstable, while the small RNA, which was similar in size to *ermC* mRNA, was relatively stable (8-min half-life, as determined by densitometry scanning). At the zero time

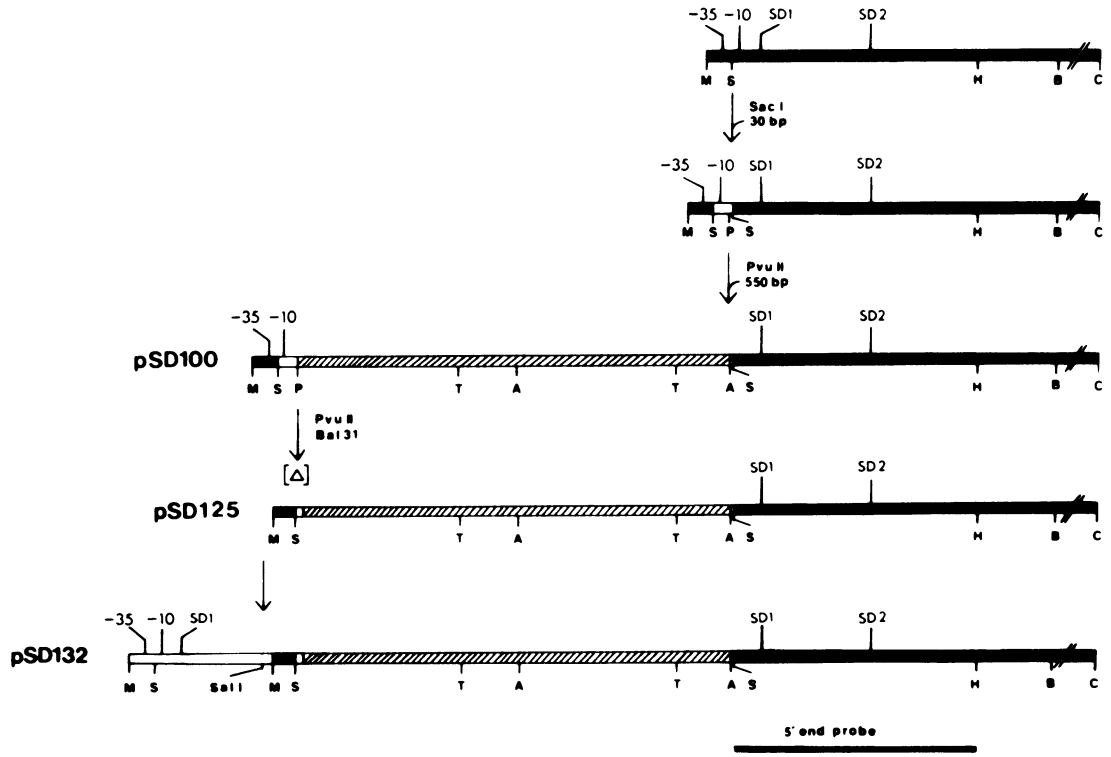

FIG. 2. Construction of pSD100 and derivatives. The *ermC* gene is represented by the solid bar at the top. Single letters denote relevant restriction endonuclease sites (A, *Alu*I; B, *Bcl*I; C, *Cla*I; H, *Hae*III; M, *Mbo*I; P, *Pvu*II; S, *Sac*I; T, *Taq*I). The *ermC* promoter is indicated by −35 and −10 at the left; transcription terminates upstream of the *Cla*I site (22; D. H. Bechhofer, unpublished data). The open box in the second line indicates the synthetic 30-base-pair (bp) fragment containing a *Pvu*II site, which was cloned into the *Sac*I site. The hatched bar in pSD100 indicates the 550-base-pair insert consisting of tandem 275-base-pair *Alu*I fragments; the 550-base-pair insert was cloned into the *Pvu*II site. The triangle above the diagram of pSD125 denotes the *Bal* 31-generated, 25-base-pair deletion of pSD100. Construction of pSD132 is described in the text. The location of the 5′ end probe, which was used in Northern blot experiments, is shown at the lower right.

point after rifampin addition, the probe also detected unstable RNA fragments of intermediate size.

To demonstrate that the small RNA was a processed product of the large RNA and was not being transcribed from a promoter within the 550-base-pair insert, RNA from the pSD100 strain was probed with DNA complementary to the inserted *Alu*I fragment. Only the large RNA was detected by this upstream probe, indicating that the small RNA is not transcribed from a promoter within the inserted DNA (data not shown). In addition, the promoter for the large RNA was inactivated by a *Bal* 31 deletion from the *Pvu*II site, which removed 15 nucleotides upstream and 10 nucleotides downstream of the *Pvu*II site (pSD125, Fig. 2). The RNA encoded by the *Bal* 31 deletion plasmid was probed with the 5′ end probe (Fig. 3C). Neither the large nor the small RNA was detected by the *ermC* probe, demonstrating that the small RNA is not transcribed from a different promoter. Therefore, the small RNA must be a processed product of the large RNA.

RNA processing to the ribosome stall site occurs with a different upstream sequence. An unstable large RNA and a stable small RNA in the presence of erythromycin could be explained if the 5′ end of *ermC* mRNA is the initiation site for decay. In the presence of erythromycin, there is a backup of stalled ribosomes from the leader peptide sequence to SD1, which is located 580 nucleotides downstream of the 5′ end of pSD100-encoded *ermC* mRNA. An RNase, possibly a 5′-to-3′ exoribonuclease or an endonuclease that binds at the 5′ end and tracks in the 5′-to-3′ direction, attacks the unprotected 5′ end and degrades this mRNA up to the site of the stalled ribosome, producing the small RNA. If this model is correct, then any RNA having an internal ribosome stall site should be processed in the same way as pSD100-encoded *ermC* mRNA. To test this, we analyzed RNA encoded by a construct that had a different sequence upstream of the *ermC* ribosome stall site.

Plasmid pBD362 is a low-copy-number version of pBD118, which was constructed previously (deletion 14 [23]). Plasmid pBD362 has a 28-base-pair deletion around the *ermC*-proximal *Sac*I site that inactivates the *ermC* promoter but leaves SD1 intact. In plasmid pBD362, *ermC* was transcribed from a promoter located approximately 1,100 nucleotides upstream of SD1 (Fig. 4A). These 1,100 nucleotides were derived from pUB110 and pE194 DNA and were not related to the pC194 DNA that constituted the 550-nucleotide insert in pSD100. Methylase synthesis in a strain carrying pBD362 is inducible by erythromycin, so that ribosome stalling occurs normally in this construct (23). RNA isolated from the pBD362 strain and probed with the 5′ end probe revealed an unstable, large (2,000-nucleotide) RNA and a small (900-nucleotide) RNA that was relatively stable (5-min half-life) in the presence of erythromycin (Fig. 4A). This small RNA was similar in size to *ermC* mRNA, as was the small RNA from the pSD100 strain. Two unstable, intermediate-sized RNAs were also detected against a background smear at the zero time point after rifampin addition. Control experiments with a plasmid deleted for the upstream promoter in pBD362 proved that the small RNA detected in the

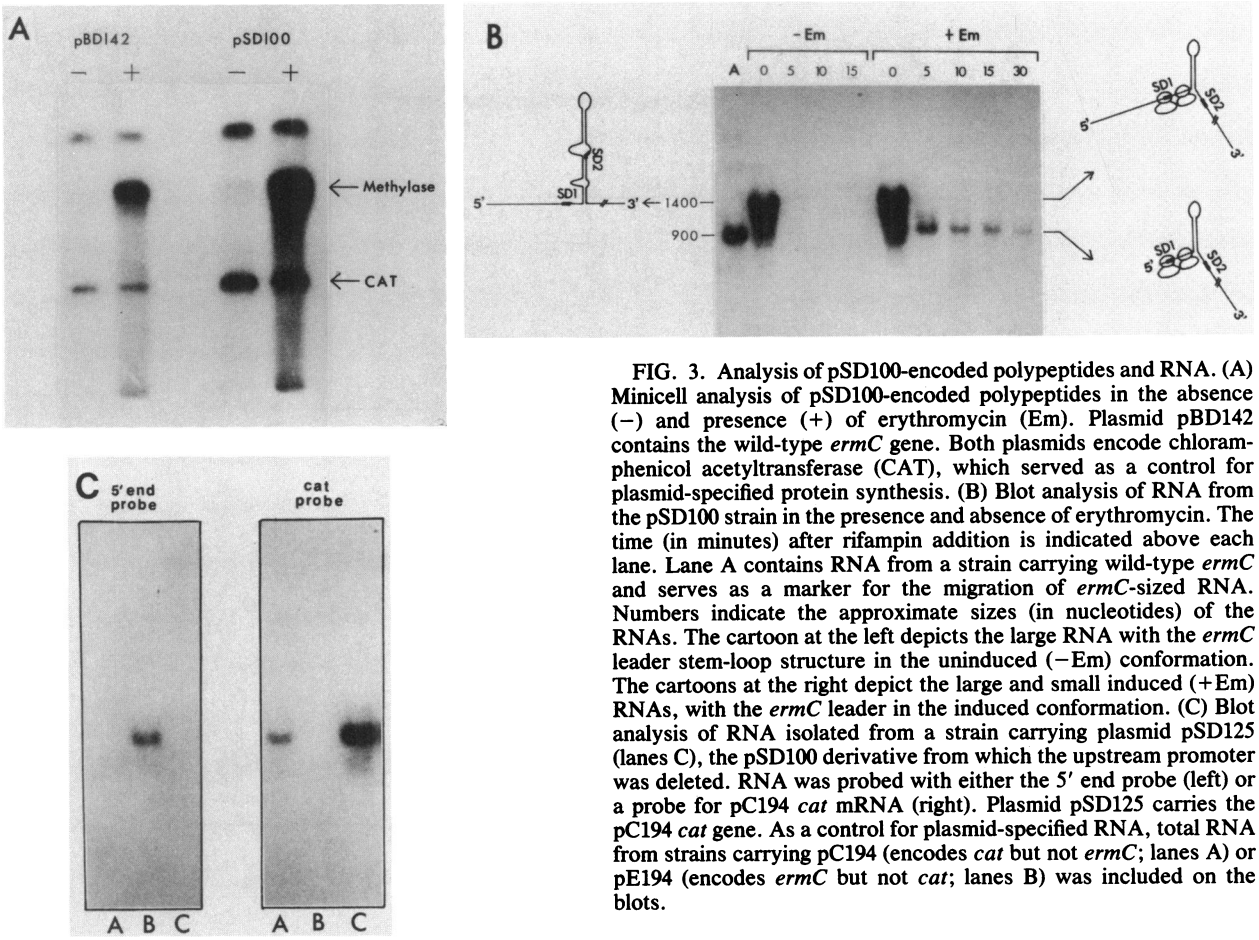

FIG. 3. Analysis of pSD100-encoded polypeptides and RNA. (A) Minicell analysis of pSD100-encoded polypeptides in the absence (−) and presence (+) of erythromycin (Em). Plasmid pBD142 contains the wild-type *ermC* gene. Both plasmids encode chloramphenicol acetyltransferase (CAT), which served as a control for plasmid-specified protein synthesis. (B) Blot analysis of RNA from the pSD100 strain in the presence and absence of erythromycin. The time (in minutes) after rifampin addition is indicated above each lane. Lane A contains RNA from a strain carrying wild-type *ermC* and serves as a marker for the migration of *ermC*-sized RNA. Numbers indicate the approximate sizes (in nucleotides) of the RNAs. The cartoon at the left depicts the large RNA with the *ermC* leader stem-loop structure in the uninduced (−Em) conformation. The cartoons at the right depict the large and small induced (+Em) RNAs, with the *ermC* leader in the induced conformation. (C) Blot analysis of RNA isolated from a strain carrying plasmid pSD125 (lanes C), the pSD100 derivative from which the upstream promoter was deleted. RNA was probed with either the 5′ end probe (left) or a probe for pC194 *cat* mRNA (right). Plasmid pSD125 carries the pC194 *cat* gene. As a control for plasmid-specified RNA, total RNA from strains carrying pC194 (encodes *cat* but not *ermC*; lanes A) or pE194 (encodes *ermC* but not *cat*; lanes B) was included on the blots.

pBD362 strain is not transcribed from an *ermC*-proximal promoter (data not shown). Thus, in the presence of erythromycin, pSD100-encoded and pBD362-encoded large RNAs, which contained different nucleotide sequences upstream of the ribosome stall site, are processed to yield similarly sized small RNAs.

Analysis of RNA in a mutant deleted for SD1. To prove that the appearance of the small RNA in the presence of erythromycin is a function of ribosome stalling and not some other effect of erythromycin addition, we examined RNA isolated from a strain carrying plasmid pBD178 (deletion 83 [23]). Plasmid pBD178 was identical to plasmid pBD362 except for a deletion of an additional 28 base pairs of the *ermC* 5′ end. This deletion included part of the SD1 sequence, and methylase synthesis was not inducible in the strain carrying pBD178 because ribosomes could not translate the leader peptide.

RNA was isolated from the strain carrying pBD178 and probed with the 5′ end probe (Fig. 4B). Unlike the results with pBD362, only a large RNA that was unstable in the presence and absence of erythromycin could be detected. Since inactivation of SD1 alone resulted in the loss of the small RNA, we conclude that translation from SD1 and subsequent ribosome stalling are required for generating the small RNA.

Mapping the 5′ ends of the processed small RNAs. Reverse transcriptase analysis was used to map the 5′ ends of the small RNAs that were detected by Northern blot analysis. RNA isolated from the pSD100 and pBD362 strains at 10 min after rifampin addition in the presence of erythromycin was used as a template for an oligonucleotide annealed to the leader peptide sequence. The data presented in Fig. 5 reveal that the 5′ ends of the stable, small RNAs mapped to the same site, which was 57 to 58 nucleotides upstream of SD1. The fact that the 5′ ends of both small RNAs were the same distance from SD1, even though the sequences upstream of SD1 in pSD100 and pBD362 were different, fits well with our working model. A sequence-independent degradation of the large RNAs begins at the 5′ end and continues downstream until its progress is blocked by a stalled ribosome.

The appearance of the small RNA could also be explained by endonucleolytic cleavage that does not require initiation at the 5′ end, followed by rapid 3′-to-5′ exonucleolytic degradation. Two modes of endonucleolytic attack that could account for the presence of stable, small RNAs were considered: (i) nonspecific endonucleolytic cleavages in the upstream sequence, followed by 3′-to-5′ exonucleolytic decay, and (ii) specific endonucleolytic cleavage at the site 57 to 58 nucleotides from SD1, followed by rapid 3′-to-5′ exonucleolytic decay of the upstream RNA. Although the sequences at that site were different in pSD100 and pBD362, it was possible that the presence of a stalled ribosome triggered an endonucleolytic cleavage adjacent to it. The experiment described in the next section was designed to eliminate these two possibilities.

An RNA with two ribosome stall sites. To prove that the small RNA was generated by a ribonucleolytic decay proceeding from the 5′ end and not by endonucleolytic cleavage, we constructed a derivative of pSD100 that had an

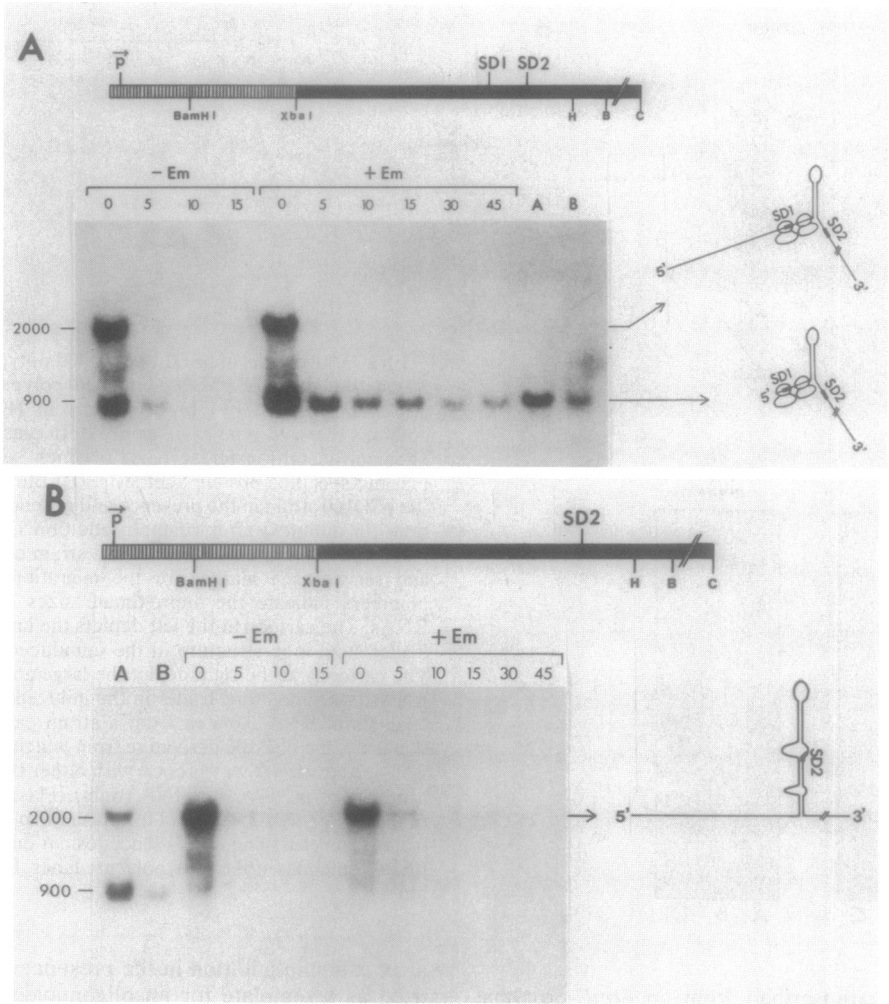

FIG. 4. Blot analysis of RNAs with a 1,100-nucleotide 5′ extension. (A) Blot analysis of RNA from the pBD362 strain in the presence and absence of erythromycin (Em). The diagram on top represents the relevant portion of plasmid pBD362. Vertical lines indicate pUB110 sequences; the solid bar indicates pE194 sequences. Approximate location of the upstream promoter (p) and restriction sites (H, *Hae*III; B, *Bcl*I; C, *Cla*I) is shown. The cartoons at the right of the blot depict the induced large and small RNAs. Numbers above the lanes are times (in minutes). Lane A, RNA from the pE194 (wild-type *ermC*) strain; lane B, RNA from the pSD100 strain at 10 min after rifampin addition in the presence of erythromycin. Numbers to the left of the gel indicate the approximate sizes (in nucleotides) of the RNAs. (B) Blot analysis of RNA from the strain carrying pBD178, which did not have a functional SD1 sequence. The diagram on top is the same as that in panel A, except for the deletion of SD1 sequences. The cartoon at the right depicts the unstable large RNA. Lanes A and B, RNA from the pBD362 strain at 0 and 10 min, respectively, after rifampin addition in the presence of erythromycin.

additional *ermC* ribosome stall site at the 5′ end of the large RNA. If the small RNA species from pSD100 resulted from endonucleolytic cleavage, then the same RNA pattern (an unstable large RNA and a stable small RNA) should be observed in a strain carrying a plasmid which encodes an RNA that has ribosomes stalled both at the 5′ end and internally. However, if the small RNA is the result of decay initiating at the 5′ end, then the presence of a stalled ribosome at the 5′ end would block this decay and only a large, stable RNA would be observed.

From experiments with deletion mutants in the *ermC* leader region, we know that the leader peptide-coding sequence alone, without the entire *ermC* leader stem-loop structure, is sufficient to allow ribosome stalling in the presence of erythromycin (K. K. Hue and D. H. Bechhofer, unpublished data). A small DNA fragment that contained the first 90 base pairs of *ermC*, including SD1 and the leader peptide sequence, was cloned upstream of the inserted *Alu*I fragments in pSD100 to yield plasmid pSD132 (Fig. 2; see Materials and Methods). Methylase expression from pSD132 was inducible by erythromycin, indicating that ribosome stalling occurs normally at the internal stall site.

RNA was isolated from the strain carrying pSD132, in the presence and absence of erythromycin. As can be seen from the Northern blot analysis in Fig. 6, in the presence of erythromycin the major RNA species that was detected was the large RNA. This was the full-length RNA which was stable because of the presence of a stalled ribosome at the 5′ end. The amount of the large RNA was greater than that of the other RNA species detected (compare with Fig. 3B), a result that was not expected if rapid endonucleolytic processing of the large RNA occurred. This result indicates that the small RNA is generated by a processive decay from the 5′ end and not by endonucleolytic cleavage.

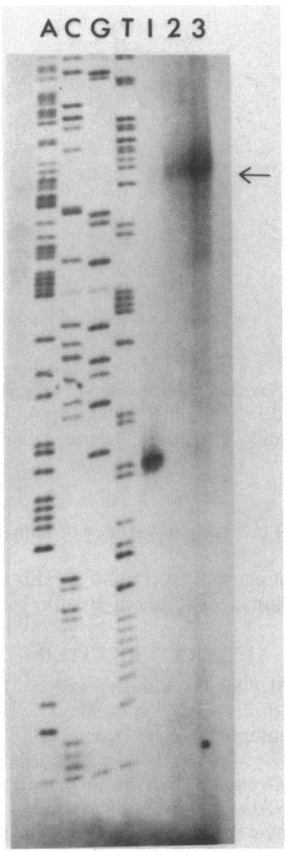

FIG. 5. Reverse transcriptase mapping of stable, small RNAs. Reverse transcriptase was used to extend an oligonucleotide primer annealed to the *ermC* leader peptide sequence. RNA was isolated from a strain containing wild-type *ermC* (lane 1) and from strains carrying plasmid pSD100 (lane 2) and plasmid pBD362 (lane 3) at 10 min after rifampin addition in the presence of erythromycin. The four left lanes are a dideoxy sequencing ladder of the *ermC* leader region with the same oligonucleotide primer as was used in the reverse transcriptase reactions. The template for the sequencing reactions was M13 single-stranded DNA containing the coding strand of the *MboI-BclI* fragment from pSD100 (see Fig. 2). The arrow marks the positions of the 5′ ends of pSD100 and pBD362 RNAs, which were 57 to 58 nucleotides upstream of SD1.

DISCUSSION

We studied the inducibly stable *ermC* mRNA in *B. subtilis* in order to probe the mechanism of decay in this organism. Earlier work has demonstrated that induced *ermC* mRNA stability results from the stalling of a ribosome in the *ermC* leader peptide sequence (3). In this report, our working hypothesis to explain erythromycin-induced *ermC* mRNA stability was that a ribosome stalled in the *ermC* leader peptide causes another ribosome, which is loading at the 5′-proximal ribosome-binding site (SD1), to stall. The ribosome stalled at SD1 covers the 5′ end of the message, which is the target for initiation of decay. If the 5′ end of the message is the target, then the enzymatic activity involved in *ermC* mRNA decay would be either a 5′-to-3′ exoribonuclease or an endoribonuclease that must bind at the 5′ end and track in the 5′-to-3′ direction.

The results presented here are consistent with this model. In RNA molecules that had the *ermC* ribosome stall site positioned internally rather than at the 5′ end, sequences upstream of the stall site were unstable in the presence of erythromycin, while downstream sequences, starting from 57 to 58 nucleotides 5′ to SD1, were stable in the presence of erythromycin. Deletion of the internal SD1 resulted in the instability of the entire RNA. In an RNA molecule that had two ribosome stall sites, one at the 5′ end and one internally, the full-length RNA was stable in the presence of erythromycin. The latter result is important because it is inconsistent with the explanation that endonucleolytic cleavage of the untranslated upstream sequences is the basis for the differential stability of the upstream and downstream RNAs. Furthermore, if endonucleolytic cleavage is responsible for the rapid decay of upstream sequences, we could not explain why the downstream sequences were not also cleaved endonucleolytically. Although the upstream sequences were not translated and the downstream sequences were, we showed that induced *ermC* mRNA stability occurs even in the absence of methylase translation (3; K. K. Hue and D. H. Bechhofer, unpublished data).

The induced half-lives of the small RNAs (5 to 8 min) were less than the induced half-life of wild-type *ermC* mRNA (40 min). If, as the results suggest, the small RNA was generated by processing from the 5′ end, this shorter half-life could be explained. We speculate that in the wild type, since the 5′ end of the message is only 9 nucleotides away from SD1, a stalled ribosome at SD1 does not allow a 5′-end-requiring RNase to begin degrading the mRNA, resulting in an extremely long half-life. In the case of pSD100 and pBD362, however, ribonucleolytic activity began at the unprotected end of the 5′-extended *ermC* mRNA. This degradation was slowed but not stopped at the site of ribosome stalling, yielding a shorter half-life than that of the induced wild type.

Probing of RNAs encoded by pSD100 and pBD362 revealed, in addition to the prominent large and small RNAs, a smear of intermediate-sized RNAs, including some that were distinguishable against the background (Fig. 3B and 4A). Even in the absence of erythromycin, *ermC*-sized mRNAs were detected shortly after rifampin addition. If a processive RNase was responsible for the decay of *ermC* mRNA, then the decay intermediates detected in the pBD362 strain could represent pausing at RNase-resistant sites. S1 nuclease mapping of these intermediates should show whether the 5′ ends of these RNAs correspond to regions of predicted secondary structure. The *ermC*-sized RNA detected at the zero time point in the absence of erythromycin could be explained by the fact that RNase paused at the *ermC* leader stem-loop structure, which is very stable (23), or by the protective effect of ribosomes that initiated translation at SD1.

It was surprising at first to find that the 5′ ends of the small RNAs were as much as 57 to 58 nucleotides upstream of SD1. Assuming that the 5′ ends of these RNAs were due to protection by a ribosome stalled at SD1, we expected, based on protection of mRNA and poly(U) by ribosome binding (26, 45), that perhaps 20 nucleotides upstream of SD1 might be protected. However, it should be noted that in these studies endoribonucleases were used to determine the extent of the message that was ribosome-bound. The protected mRNA fragments, therefore, represent only the part of the message that is bound within the mRNA trough of the 30S particle (see reference 17 for a review of mRNA-ribosome interactions). When 3′-to-5′ exoribonucleases were used in ribosome protection assays, much larger protected fragments were detected (10), probably because the mRNA that was external to the mRNA trough came into contact with other areas of the ribosome. Therefore, the RNase responsible for *ermC* mRNA decay, which we believe must pro-

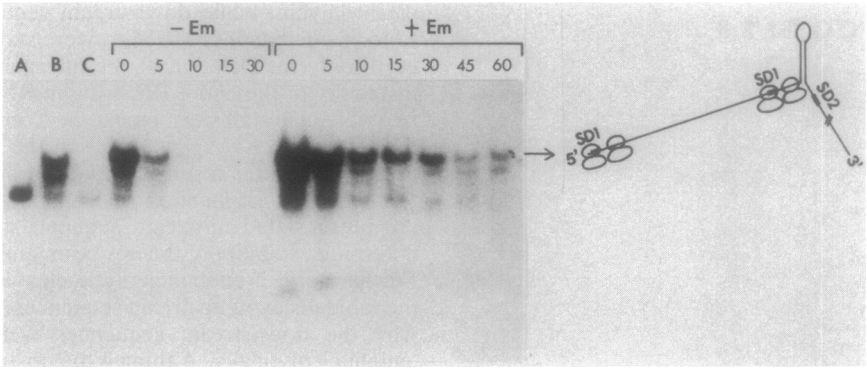

FIG. 6. Blot analysis of RNA from the pSD132 strain. Plasmid pSD132 encoded an mRNA that contained two ribosome stall sites, one at the 5′ end of the message and one internally. The cartoon at the right depicts the induced full-length RNA. Lane A, RNA from a pE194 (wild-type *ermC*) strain; lanes B and C, RNAs from the pSD100 strain, isolated at 0 and 5 min., respectively, after rifampin addition in the presence of erythromycin (Em) (see Fig. 3B).

ceed in the 5′-to-3′ direction, may encounter an mRNA-ribosome interaction well upstream of SD1.

It is also possible that protection of sequences upstream of SD1 is due to ribosome binding at sites other than SD1. However, a computer search of the upstream sequences in pSD100 and pBD362 did not reveal any reasonable ribosome-binding sites followed by open reading frames that could deliver a ribosome to the region upstream of SD1. Likewise, open reading frames were not found in the upstream sequence of plasmid pSD132, the construct with 5′-terminal and internal ribosome stall sites. A computer search for possible stem-loop structures (13) that could be involved in protecting downstream sequences from exonucleolytic processing did not predict any strong secondary structure for the region to which the 5′ ends of the small RNAs were mapped.

It has been reported that the 3′ end of the *Bacillus thuringiensis cry* gene, which encodes a relatively stable mRNA, enhances the stability of heterologous messages when inserted at their 3′ ends in both *B. subtilis* and *E. coli* (50). These investigators concluded that mRNA decay in *B. subtilis* occurs by a 3′-to-5′ exonuclease. On the other hand, our previous results show that the *ermC* 5′ 360 nucleotides confers *cis*-dominant stability to diverse downstream sequences (3). If 3′-to-5′ exonucleases are a major factor in mRNA decay in *B. subtilis*, it is not clear how the presence of *ermC* 5′ sequences at the 5′ end of an RNA would affect decay initiating at the 3′ end.

An early report of a 5′-to-3′ exoribonuclease activity in *E. coli* (30) was questioned a short time later (7, 24). Since then, it has been assumed that mRNA turnover in bacteria is accomplished by 3′-to-5′ exoribonucleases that initiate decay either at the 3′ end of the message or at 3′ ends generated by prior endonucleolytic cleavages. It would be of interest to examine the decay of *ermC* mRNA in *E. coli*, since *ermC* is expressed and somewhat inducible in *E. coli* (28, 47).

In conclusion, our results indicate that the decay of *ermC* mRNA in *B. subtilis* occurs either by a 5′-to-3′ exonuclease or by an endonuclease that tracks in the 5′-to-3′ direction from the 5′ end. Biochemical identification of such an activity in *B. subtilis* extracts is necessary to confirm this conclusion.

ACKNOWLEDGMENTS

We thank David Dubnau for scientific advice and *B. subtilis* strains. We thank David Figurski for critical reading of the manuscript. The excellent technical assistance of Kim K. Hue is acknowledged.

This work was supported by Public Health Service grant GM-39516 from the National Institutes of Health.

LITERATURE CITED

1. **Arraiano, C. M., S. D. Yancey, and S. R. Kushner.** 1988. Stabilization of discrete mRNA breakdown products in *ams pnp rnb* multiple mutants of *Escherichia coli* K-12. J. Bacteriol. **170**:4625–4633.
2. **Baga, M., M. Gransson, S. Normark, and B. E. Uhlin.** 1988. Processed mRNA with differential stability in the regulation of *E. coli* pilin gene expression. Cell **52**:197–206.
3. **Bechhofer, D. H., and D. Dubnau.** 1987. Induced mRNA stability in *Bacillus subtilis*. Proc. Natl. Acad. Sci. USA **84**:498–502.
4. **Belasco, J. G., J. T. Beatty, C. W. Adams, A. von Gabain, and S. N. Cohen.** 1985. Differential expression of photosynthesis genes in *R. capsulata* results from segmental differences in stability within the polycistronic *rxcA* transcript. Cell **40**:171–181.
5. **Belasco, J. G., G. Nilsson, A. von Gabain, and S. N. Cohen.** 1986. The stability of *E. coli* gene transcripts is dependent on determinants localized to specific mRNA segments. Cell **46**:245–251.
6. **Belin, D., E. A. Mudd, P. Prentki, Y. Yi-Yi, and H. M. Krisch.** 1987. Sense and antisense transcription of bacteriophage T4 gene *32*. J. Mol. Biol. **194**:231–243.
7. **Bothwell, A. L. M., and D. Apirion.** 1971. Is RNase V a manifestation of RNase II? Biochem. Biophys. Res. Commun. **44**:844–851.
8. **Brawerman, G.** 1987. Determinants of messenger RNA stability. Cell **48**:5–6.
9. **Cannistraro, V. J., M. N. Subbarao, and D. Kennell.** 1986. Specific endonucleolytic cleavage sites for decay of *Escherichia coli* mRNA. J. Mol. Biol. **192**:257–274.
10. **Castles, J. J., and M. F. Singer.** 1969. Degradation of polyuridylic acid by ribonuclease II: protection by ribosomes. J. Mol. Biol. **40**:1–17.
11. **Chen, C.-Y. A., J. T. Beatty, S. N. Cohen, and J. G. Belasco.** 1988. An intercistronic stem-loop structure functions as an mRNA decay terminator necessary but insufficient for *puf* mRNA stability. Cell **52**:609–619.
12. **Deutscher, M. P.** 1985. *E. coli* RNases: making sense of alphabet soup. Cell **40**:731–732.
13. **Devereux, J., P. Haeberli, and O. Smithies.** 1984. A comprehensive set of sequence analysis programs for the VAX. Nucleic Acids Res. **12**:387–395.
14. **Donovan, W. P., and S. R. Kushner.** 1986. Polynucleotide phosphorylase and ribonuclease II are required for cell viability and mRNA turnover in *Escherichia coli* K-12. Proc. Natl. Acad. Sci. USA **83**:120–124.
15. **Dubnau, D.** 1984. Translational attenuation: the regulation of

bacterial resistance to the macrolide-lincosamide-streptogramin B antibiotics. Crit. Rev. Biochem. **16**:103–132.
16. **Dubnau, D., and R. Davidoff-Abelson.** 1971. Fate of transforming DNA following uptake by competent *Bacillus subtilis*. I. Formation and properties of the donor-recipient complex. J. Mol. Biol. **56**:209–221.
17. **Gold, L.** 1988. Posttranscriptional regulatory mechanisms in *Escherichia coli*. Annu. Rev. Biochem. **57**:199–233.
18. **Gorski, K., J.-M. Roch, P. Prentki, and H. M. Krisch.** 1985. The stability of bacteriophage T4 gene *32* mRNA: a 5′ leader sequence that can stabilize mRNA transcripts. Cell **43**:461–469.
19. **Graves, M. C., and J. C. Rabinowitz.** 1986. *In vivo* and *in vitro* transcription of the *Clostridium pasteurianum* ferredoxin gene. J. Biol. Chem. **261**:11409–11415.
20. **Gryczan, T. J., S. Contente, and D. Dubnau.** 1978. Characterization of *Staphylococcus aureus* plasmids introduced by transformation into *Bacillus subtilis*. J. Bacteriol. **134**:318–329.
21. **Gryczan, T. J., G. Grandi, J. Hahn, S. Contente, and D. Dubnau.** 1982. Replication and incompatibility properties of plasmid pE194 in *Bacillus subtilis*. J. Bacteriol. **152**:722–735.
22. **Gryczan, T. J., G. Grandi, J. Hahn, R. Grandi, and D. Dubnau.** 1980. Conformational alteration of mRNA structure and the posttranscriptional regulation of erythromycin-induced drug resistance. Nucleic Acids Res. **8**:6081–6097.
23. **Hahn, J., G. Grandi, T. J. Gryczan, and D. Dubnau.** 1982. Translational attenuation of *ermC*: a deletion analysis. Mol. Gen. Genet. **186**:204–216.
24. **Holmes, R. K., and M. F. Singer.** 1971. Inability to detect RNase V in *Escherichia coli* and comparison of other ribonucleases before and after infection with coliphage T7. Biochem. Biophys. Res. Commun. **44**:837–843.
25. **Horinouchi, S., and B. Weisblum.** 1982. Nucleotide sequence and functional map of pC194, a plasmid that specifies chloramphenicol resistance. J. Bacteriol. **150**:815–825.
26. **Kang, C., and C. R. Cantor.** 1985. Structure of ribosome-bound messenger RNA as revealed by enzymatic accessibility studies. J. Mol. Biol. **181**:241–251.
27. **King T. C., R. Sirdeskmukh, and D. Schlessinger.** 1986. Nucleolytic processing of ribonucleic acid transcripts in procaryotes. Microbiol. Rev. **50**:428–451.
28. **Kirsch, D. R., and M. H. Lai.** 1984. Regulation of a macrolide resistance–β-galactosidase (*ermC-lacZ*) gene fusion in *Escherichia coli*. J. Bacteriol. **159**:381–384.
29. **Kunkel, T. A., J. D. Roberts, and R. A. Zakour.** 1987. Rapid and efficient mutagenesis without phenotypic selection. Methods Enzymol. **154**:367–382.
30. **Kuwano, M., D. Schlessinger, and D. Apirion.** 1970. Ribonuclease V of *Escherichia coli*. J. Mol. Biol. **51**:75–82.
31. **Lundberg, U., G. Nilsson, and A. von Gabain.** 1988. The differential stability of the *Escherichia coli ompA* and *bla* mRNA at various growth rates is not correlated to the efficiency of translation. Gene **72**:141–149.
32. **Mayford, M., and B. Weisblum.** 1989. *ermC* leader peptide: amino acid sequence critical for induction by translational attenuation. J. Mol. Biol. **206**:69–79.
33. **Melefors, Ö., and A. von Gabain.** 1988. Site-specific endonucleolytic cleavages and the regulation of stability of *E. coli ompA* mRNA. Cell **52**:893–901.
34. **Mudd, E. A., P. Prentki, D. Belin, and H. M. Krisch.** 1988. Processing of unstable bacteriophage T4 gene *32* mRNAs into a stable species requires *Escherichia coli* ribonuclease E. EMBO J. **7**:3601–3607.
35. **Narayanan, C. S., and D. Dubnau.** 1985. Evidence for the translational attenuation model: ribosome-binding studies and structural analysis with an *in vitro* run-off transcript of *ermC*. Nucleic Acids Res. **13**:7307–7325.
36. **Narayanan, C. S., and D. Dubnau.** 1987. Demonstration of erythromycin-dependent stalling of ribosomes on the *ermC* leader transcript. J. Biol. Chem. **262**:1766–1771.
37. **Newbury, S. F., N. H. Smith, and C. F. Higgins.** 1987. Differential mRNA stability controls relative gene expression within a polycistronic operon. Cell **51**:1131–1143.
38. **Nilsson, G., U. Lundberg, and A. von Gabain.** 1988. *In vivo* and *in vitro* identity of site specific cleavages in the 5′ non-coding region of *ompA* and *bla* mRNA in *Escherichia coli*. EMBO J. **7**:2269–2275.
39. **Portier, C., L. Dondon, M. Grunberg-Manago, and P. Régnier.** 1987. The first step in the functional inactivation of the *Escherichia coli* polynucleotide phosphorylase messenger is a ribonuclease III processing at the 5′ end. EMBO J. **6**:2165–2170.
40. **Reeve, J. N., N. H. Mendelson, S. I. Coyne, L. L. Hallock, and R. M. Cole.** 1973. Minicells of *Bacillus subtilis*. J. Bacteriol. **114**:860–873.
41. **Sandler, P., and B. Weisblum.** 1988. Erythromycin-induced stabilization of *ermA* messenger RNA in *Staphylococcus aureus* and *Bacillus subtilis*. J. Mol. Biol. **203**:905–915.
42. **Shivakumar, A. G., and D. Dubnau.** 1981. Characterization of a plasmid-specified ribosome methylase associated with macrolide resistance. Nucleic Acids Res. **9**:2549–2562.
43. **Shivakumar, A. G., J. Hahn, and D. Dubnau.** 1979. Studies on the synthesis of plasmid-coded proteins and their control in *Bacillus subtilis* minicells. Plasmid **2**:279–289.
44. **Shivakumar, A. G., J. Hahn, G. Grandi, Y. Kozlov, and D. Dubnau.** 1980. Posttranscriptional regulation of an erythromycin resistance protein specified by plasmid pE194. Proc. Natl. Acad. Sci. USA **77**:3903–3907.
45. **Steitz, J. A.** 1969. Polypeptide chain initiation: nucleotide sequences of the three ribosomal binding sites in bacteriophage R17 RNA. Nature (London) **224**:957–964.
46. **Subbarao, M. N., and D. Kennell.** 1988. Evidence for endonucleolytic cleavages in decay of *lacZ* and *lacI* mRNAs. J. Bacteriol. **170**:2860–2865.
47. **Thakker-Varia, S., A. C. Ranzini, and D. T. Dubin.** 1985. Ribosomal RNA methylation in *Staphylococcus aureus* and *Escherichia coli*: effect of the "MLS" (erythromycin resistance) methylase. Plasmid **14**:152–161.
48. **Weisblum, B.** 1983. Inducible resistance to macrolides, lincosamides and streptogramin type B antibiotics: the resistance phenotype, its biological diversity, and structural elements that regulate expression, p. 91–121. *In* J. Beckwith, J. Davies, and J. A. Gallant (ed.), Gene function in prokaryotes. Cold Spring Harbor Laboratory, Cold Spring Harbor, N.Y.
49. **Weisblum, B., C. Siddhikol, C. J. Lai, and V. Demohn.** 1971. Erythromycin-inducible resistance in *Staphylococcus aureus*: requirements for induction. J. Bacteriol. **106**:835–847.
50. **Wong, H. C., and S. Chang.** 1986. Identification of a positive retroregulator that stabilizes mRNAs in bacteria. Proc. Natl. Acad. Sci USA **83**:3233–3237.